

Protective Role of Limitrin in Experimental Autoimmune Optic Neuritis

Bo Young Chun,^{1,2} Jong-Heon Kim,^{2,3} Youn-Kwan Jung,⁴ Yoon Seok Choi,¹ Gunwoo Kim,⁵ Tomoko Yonezawa,⁶ and Kyoungho Suk^{2,3}

¹Department of Ophthalmology, School of Medicine, Kyungpook National University, Daegu, Korea

²Brain Science & Engineering Institute, School of Medicine, Kyungpook National University, Daegu, Korea

³Department of Pharmacology, School of Medicine, Kyungpook National University, Daegu, Korea

⁴Biomedical Research Institute, Gyeongsang National University Hospital, Jinju, Korea

⁵Fatima Research Institute, Fatima Hospital, Daegu, Korea

⁶Graduate School of Medicine, Dentistry and Pharmaceutical Sciences, Okayama University, Okayama, Japan

Correspondence: Bo Young Chun, Department of Ophthalmology, Brain Science & Engineering Institute, School of Medicine, Kyungpook National University, 680 Gukchaebosang St, Jung-gu, Daegu 700-422, South Korea; byjun424@hotmail.com.

BYC and JHK contributed equally to this work and should be considered equivalent authors.

Received: March 26, 2021

Accepted: June 1, 2021

Published: July 7, 2021

Citation: Chun BY, Kim J-H, Jung Y-K, et al. Protective role of limitrin in experimental autoimmune optic neuritis. *Invest Ophthalmol Vis Sci.* 2021;62(9):8. <https://doi.org/10.1167/iovs.62.9.8>

PURPOSE. This study investigated the role of limitrin in the pathogenesis of demyelinating optic neuritis using an experimental autoimmune optic neuritis (EAON) model.

METHODS. EAON was induced in mice via subcutaneous injection with myelin oligodendrocyte glycoprotein peptide. Limitrin protein and mRNA expression were examined in the optic nerve before and after EAON induction. Proinflammatory cytokine expression profiles and degree of glial activation were compared between wild-type (WT) and limitrin knockout mice by real-time PCR and histologic analysis, respectively, after EAON induction. Plasma limitrin levels in patients with optic neuritis and healthy controls were measured by ELISA.

RESULTS. Limitrin expression, observed in astrocytes in the optic nerve of WT mice, was lower in EAON-induced than in naïve WT mice. A comparative analysis of WT and limitrin knockout mice revealed that limitrin deficiency induced more severe neuroinflammation and glial hyperactivation in the optic nerve after EAON induction. Limitrin-deficient astrocytes were more chemotactically responsive to neuroinflammatory stimulation than WT astrocytes. Patients with optic neuritis demonstrated higher plasma limitrin levels than healthy controls ($P = 0.0001$), which was negatively correlated with visual acuity at the nadir of the optic neuritis attack ($r = 0.46$, $P = 0.036$).

CONCLUSIONS. Limitrin deficiency induced severe neuroinflammation and reactive gliosis in the optic nerve after EAON induction. Our results imply that astrocyte-derived limitrin may protect against neuroinflammation by decreasing immune cell infiltration into the optic nerve. The plasma limitrin level may reflect the extent of blood-brain barrier disruption and provide a valuable biomarker reflecting the severity of optic neuritis.

Keywords: astrocytes, blood-brain barrier, demyelinating optic neuritis, limitrin, neuroinflammation

Optic neuritis presents as an acute optic nerve inflammation with decreased visual acuity and dyschromatopsia.¹ Approximately, 20% of patients with multiple sclerosis (MS) experience optic neuritis as the initial manifestation of disease, and up to 50% of patients with MS develop optic neuritis at some point.¹ Visual acuity improves over several weeks in the majority of patients with optic neuritis; however, some level of permanent vision loss was reported in 40% of patients in the Optic Neuritis Treatment Trial.¹⁻³ Understanding the histopathology of optic neuritis is crucial for developing future neuroprotective treatments to prevent irreversible vision loss.⁴

The pathogenesis of optic neuritis is reportedly demyelination and chronic inflammation of the optic nerve axons with a relapsing and remitting course, eventually causing retinal ganglion cell damage.⁴⁻⁷ Studies using experimental autoimmune optic neuritis (EAON) animal models have reported that early infiltration of activated microglia

causes initial damage to axons, followed by infiltration of T cells, which induces demyelination of the optic nerve.^{4-6,8,9} Inflammatory demyelination leads to significant axonal loss and retinal ganglion cell death by apoptosis in experimental optic neuritis.^{4,5}

Disruption of the blood-brain barrier (BBB) and immune cell infiltration are considered the initial steps in demyelinating neuroinflammatory diseases, including MS and neuromyelitis optica.¹⁰⁻¹³ The optic nerve is a part of the central nervous system (CNS) and shares many histologic characteristics with the brain; that is, it is myelinated by oligodendrocytes and protected by three meningeal layers and the BBB.¹⁴ Contrast enhancement of the optic nerve by MRI, indicating BBB disruption, has been well-documented during an optic neuritis attack.^{14,15} However, little is known of the pathophysiology of the BBB in the optic nerve during the acute stage of optic neuritis.

BBB disruption leading to immune cell infiltration is remarkably important to the pathogenesis of demyelinating neuroinflammatory diseases of the CNS.^{10–13} The BBB is indispensable for maintaining CNS homeostasis by regulating the passage of soluble compounds and peripheral immune cells, and protecting against toxic elements and pathogens.^{10–14,16} BBB permeability is highly selective, physically established by tight junctions between endothelial cells.^{10–14,16} Highly specialized brain endothelial cells are one of the main components of the BBB, of which the inner barrier is composed of the glia limitans and its basement membrane.^{16–18} The cerebrovasculature is invested by a basement membrane surrounded by astrocytic endfeet, which also contact the basement membrane under the pia mater to form the superficial glia limitans.^{16–18} Therefore, perivascular astrocytes are a key component of the BBB and regulate its function by coupling neuronal activity to local blood flow, thus mediating homeostatic regulation of neuronal metabolism, and altering BBB permeability by regulating junctional protein expression.^{17–20}

Previously, Yonezawa et al.¹⁶ introduced limitrin, a novel protein of the immunoglobulin superfamily formed by astrocytic endfeet in the mouse brain. Limitrin, a dual Ig domain-containing cell adhesion molecule, interacts with $\alpha v \beta 3$ integrin and stabilizes the integrity of the junctional complex in the intestinal mucosal barrier under inflammatory conditions.^{21,22} Limitrin expression is highly localized to the glia limitans, which defines the morphologic border of the brain parenchyma.¹⁶ Suggested to be physically and functionally associated with the BBB, limitrin may regulate BBB function.¹⁶ However, to our knowledge, limitrin expression and its behavior have not been reported in demyelinating optic neuritis. The purpose of this study was to investigate limitrin expression in the optic nerve and to evaluate the pathophysiological role of limitrin in optic neuritis using the EAON model based on limitrin knockout (KO) mice.

METHODS

Animals

Female wild-type (WT) C57BL/6 mice (7–8 weeks of age, $n = 24$) were obtained from Samtaco (Osan, Korea). Female limitrin KO mice (7–8 weeks of age, $n = 26$) were kindly provided by Tomoko Yonezawa (Graduate School of Medicine and Dentistry, Okayama University, Japan). Limitrin KO mice were backcrossed for 8 to 10 generations on the C57BL/6 background to generate homozygous and heterozygous animals. All mice were housed in groups of three to five per cage under specific pathogen-free conditions and a 12-hour light/dark cycle. Animals used in the present study were acquired and cared for in accordance with the procedures approved by the Institutional Animal Care Committee of Kyungpook National University and the animal care guidelines of the National Institutes of Health, and in accordance with the ARVO Statement for the Use of Animals in Ophthalmic and Vision Research.

EAON Model

EAON was induced in an experimental autoimmune encephalomyelitis (EAE) mouse model (WT, $n = 12$; limitrin KO, $n = 18$), as previously described.^{4,5,23,24} Areas draining into axillary and inguinal lymph nodes of 7- to 8-week-old mice were subcutaneously injected with 200

μg myelin oligodendrocyte glycoprotein (MOG_{35–55} peptide fragment MEVGWYRSPFSRVVHLYRNGK; GL Biochem Ltd., Shanghai, China) emulsified in 100 μL solution containing 50% complete Freund's adjuvant and 10 mg/mL heat-killed H37Ra strain of *Mycobacterium tuberculosis* (Difco Laboratories, Detroit, MI). Pertussis toxin (List Biological Laboratories, Campbell, CA) dissolved in PBS (200 ng/mouse) was administered intraperitoneally on days of immunization and again 48 hours later. Animals were weighed and examined for disease symptoms daily. Evaluation of disease severity and other experiments were carried out in a blinded fashion. EAE severity was scored using a 0 to 5 grade scale as follows: grade 0 = no symptoms; grade 1 = limp tail; grade 2 = weakness and incomplete paralysis of one or two hind limbs; grade 3 = complete hind limb paralysis; grade 4 = forelimb weakness or paralysis; and grade 5 = moribund state or death. Comparison of EAON severity between WT and limitrin KO mice has performed on mice with grade 1 EAE symptoms.

Optic Nerve Histology

Mice (WT, $n = 16$; limitrin KO, $n = 20$) were euthanized with diethyl ether, transcardially perfused with cold saline, and then perfused with 4% paraformaldehyde diluted in 0.1 M PBS. Optic nerves were isolated and fixed for 1 day using 4% paraformaldehyde, and then cryoprotected with 30% sucrose solution for 3 days. Tissues were embedded in Tissue-Tek OCT compound (Sakura Finetek Inc., Tokyo, Japan), frozen, and then cut into 16- μm thick longitudinal sections.

To assess demyelination and inflammatory cell infiltration, sections were stained with hematoxylin and eosin²⁵ and FluoroMyelin (1:300 dilution; Invitrogen, Carlsbad, CA) for 20 minutes and counterstained using DAPI. To detect limitrin expression and glial activation, sections were incubated with polyclonal rabbit anti-limitrin antibody (1:200; Novus Biologicals, Milan, Italy) overnight at 4 °C. To define the limitrin-expressing cell type, sections were co-immunostained by incubating with monoclonal goat antiglial fibrillary acidic protein (GFAP) antibody (1:200; Novus Biologicals) or monoclonal goat anti-ionized calcium-binding adapter molecule-1 (Iba-1) antibody (1:200; Novus Biologicals) overnight at 4 °C, followed by visualization with Cy5-conjugated anti-rabbit IgG and FITC-conjugated anti-goat or mouse IgG antibody (Jackson Laboratory, Bar Harbor, ME) by incubating at room temperature for 2 hours.

To compare glia morphologic activation, sections were incubated with polyclonal rabbit anti-GFAP antibody (Dako, Glostrup, Denmark) or polyclonal rabbit anti-Iba-1 antibody (WAKO Pure Chemical Industries Ltd., Osaka, Japan) and visualized with Cy3-conjugated anti-rabbit IgG (Jackson Laboratory). Images of the sections were captured using a D70 CCD color video camera (Olympus, Tokyo, Japan) attached to a BX51 microscope (Olympus). Image analysis was conducted using Fiji software (<https://imagej.net/Fiji>).²⁶ Briefly, five areas (300 \times 300 pixels each) were randomly selected within the image obtained from the optic nerve of each mouse. A binary composite image was obtained from each animal via thresholding at 50% of the background level, and particles were converted to a subthreshold image (area ≤ 1000 and ≥ 5 pixels for total cells, area ≤ 1000 and ≥ 200 pixels for amoeboid-shaped cells), which were identified as Iba-1-positive cells. Binary images among the groups were adjusted using the same threshold, and cells were recognized and quantified by counting pixels. The number of

TABLE 1. DNA Sequences of the Primers Used for Real-Time PCR

Gene	Primer Sequences	GenBank Accession No.
Mouse <i>limitrin</i>	F: 5'-GCGCCGACTTGTGGATATGTA-3' R: 5'-GCCGTCGTGGAAAGCAGAA-3'	NM_024263
Mouse <i>tnf-α</i>	F: 5'-TCACACTCAGATCATCTTCTC-3' R: 5'-ATGAGATAGCAAATCGGCTG-3'	NM_013693
Mouse <i>il-1β</i>	F: 5'-CTTTGAAGAAGAGCCCATCC-3' R: 5'-TTTGTGCTTGCTTGGTTCTC-3'	NM_008361
Mouse <i>ifn-γ</i>	F: 5'-TCTCCAGAAACCCTCACTGGT-3' R: 5'-GAGGCTCTCTGCTGTCCATC-3'	NM_008330
Mouse <i>Cd68</i>	F: 5'-TGTCTGATCTGTCTAGGACCG-3' R: 5'-GAGGCTCTCTGCTGTCCATC-3'	NM_009853
Mouse <i>Ccl3</i>	F: 5'-TTCTCTGTACCATGACACTCTGC-3' R: 5'-CGTGAATCTTCCGGCTGTAG-3'	NM_011337
Mouse <i>Ccl5</i>	F: 5'-GCTGCTTTGCCTACCTCTCC-3' R: 5'-TCGAGTGACAAACACGACTGC-3'	NM_013653
Mouse <i>Cxcl10</i>	F: 5'-CCAAGTGCTGCCGTCAATTTTC-3' R: 5'-GGCTCGCAGGGATGATTTCAA-3'	NM_021274
Mouse <i>Cxcl5</i>	F: 5'-GTTCCATCTCGCCATTCATGC-3' R: 5'-GCGGCTATGACTGAGGAAGG-3'	NM_009141
Mouse <i>Gfap</i>	F: 5'-TCCTGGAACAGCAAAACAAG-3' R: 5'-CAGCCTCAGGTTGGTTTCAT-3'	NM_001131020.1
Mouse <i>gapdh</i>	F: 5'-TGGGCTACACTGAGCACCAG-3' R: 5'-GGGTGTCGCTGTTGAAGTCA-3'	NM_008084

cells was calculated and presented as an area (in millimeters squared). For GFAP-positive cells, the intensity was measured using Fiji software and presented as fold change.

Real-Time PCR

Total RNA was extracted from the optic nerve tissue using TRIzol reagent (Invitrogen), according to the manufacturer's instructions. Total RNA (0.5 μg) was reverse-transcribed into cDNA using Superscript II (Invitrogen) and oligo (dT) primers. Real-Time PCR was performed using the One Step SYBR PrimeScript RT-PCR Kit (Takara Bio Inc., Tokyo, Japan) with the ABI Prism 7500 Sequence Detection System (Applied Biosystems, Foster City, CA). Nucleotide sequences of the primers were based on published cDNA sequences (Table 1). *Gapdh* was used as a reference control.

Cell Culture

Whole brains from 3-day-old C57BL/6 mice (WT or limitrin KO) were chopped and mechanically disrupted using a nylon mesh. The mixed glial cells obtained were seeded in culture flasks and grown at 37 °C under a 5% CO₂ atmosphere in Dulbecco's modified Eagle's medium supplemented with 10% heat-inactivated fetal bovine serum, 100 U/mL penicillin, and 100 μg/mL streptomycin. The culture medium was changed initially after 5 days and then every 3 days. Cells were used after 14 to 21 days of culture. Pure astrocyte cultures were prepared by shaking mixed glial cells overnight at 240 rpm under normal cell culture conditions to detach oligodendrocyte precursor cells and microglia, as previously described.²⁷ The remaining astrocytes were trypsinized and seeded on 100-mm² plates at a density of 1 × 10⁶ cells per plate. The purity of the astrocyte culture was determined by immunocytochemical examination using antibody against GFAP protein (Supplementary Fig. S1).

Nitric Oxide and Cell Viability Assay

NO₂ concentrations in the culture media were measured to assess nitric oxide (NO) production in astrocytes using Griess reagent. For each sample, a 50-μL aliquot was mixed with 50 μL of Griess reagent (1% sulfanilamide/0.1% naphthylethylene diamine dihydrochloride/2% phosphoric acid) in a 96-well plate. NaNO₂ was used as the standard to calculate NO₂ concentrations. The absorbance at 540 nm was then measured using a SpectraMax M5 microplate reader (Molecular Devices, San Jose, CA). Cell viability was measured by MTT assay. Astrocytes were incubated with 50 μL water soluble MTT [3-(4, 5-dimethylthiazol-2-yl)-2, 5-diphenyltetrazolium bromide, 2.5 mg/mL] for 4 hours. Insoluble MTT formazan was dissolved in dimethyl sulfoxide. The absorbance at 570 nm was then measured using the microplate reader.

Limitrin Measurement in Human Plasma by ELISA

This study was conducted between September 2016 and August 2019 at the Department of Ophthalmology of the Kyungpook National University Hospital. The study was approved by the Institutional Review Board and followed the tenets of the Declaration of Helsinki. Informed consent was obtained from all participants. A total of 32 consecutive patients diagnosed with demyelinating optic neuritis were identified, among whom 21 patients were included in this study. Eleven patients with MS, neuromyelitis optica, acute disseminated encephalomyelitis, and symptomatic CNS lesions other than on the optic nerve were excluded from this study. Optic neuritis was diagnosed based on the presence of acute visual symptoms, such as acute vision loss or visual field defect consistent with optic neuropathy with a relative afferent pupillary defect in the affected eye.³ A Snellen chart was used to measure visual acuity and converted into LogMAR acuity for statistical analysis. Blood samples from 21 patients were obtained on the day of diagnosis. Blood samples were also obtained from

30 healthy controls with Snellen visual acuities of 20/20. Plasma limitrin levels were measured using a commercial Human Matrix-Remodeling-Associated Protein 8 (Limitrin) ELISA kit (Cusabio [CSB-EL015257HU], Wuhan, China) using 100 μ L plasma (1:400 dilution) per the manufacturer's instructions. All measurements were obtained from duplicate assays.

Statistical Analysis

Statistical analyses were performed using Prism software version 8.0 software (GraphPad Software, La Jolla, CA) and MedCalc version 19.0.7 software (MedCalc Software Ltd., Flanders, Belgium). All values are expressed as mean \pm SEM. The Mann-Whitney *U* test was used to

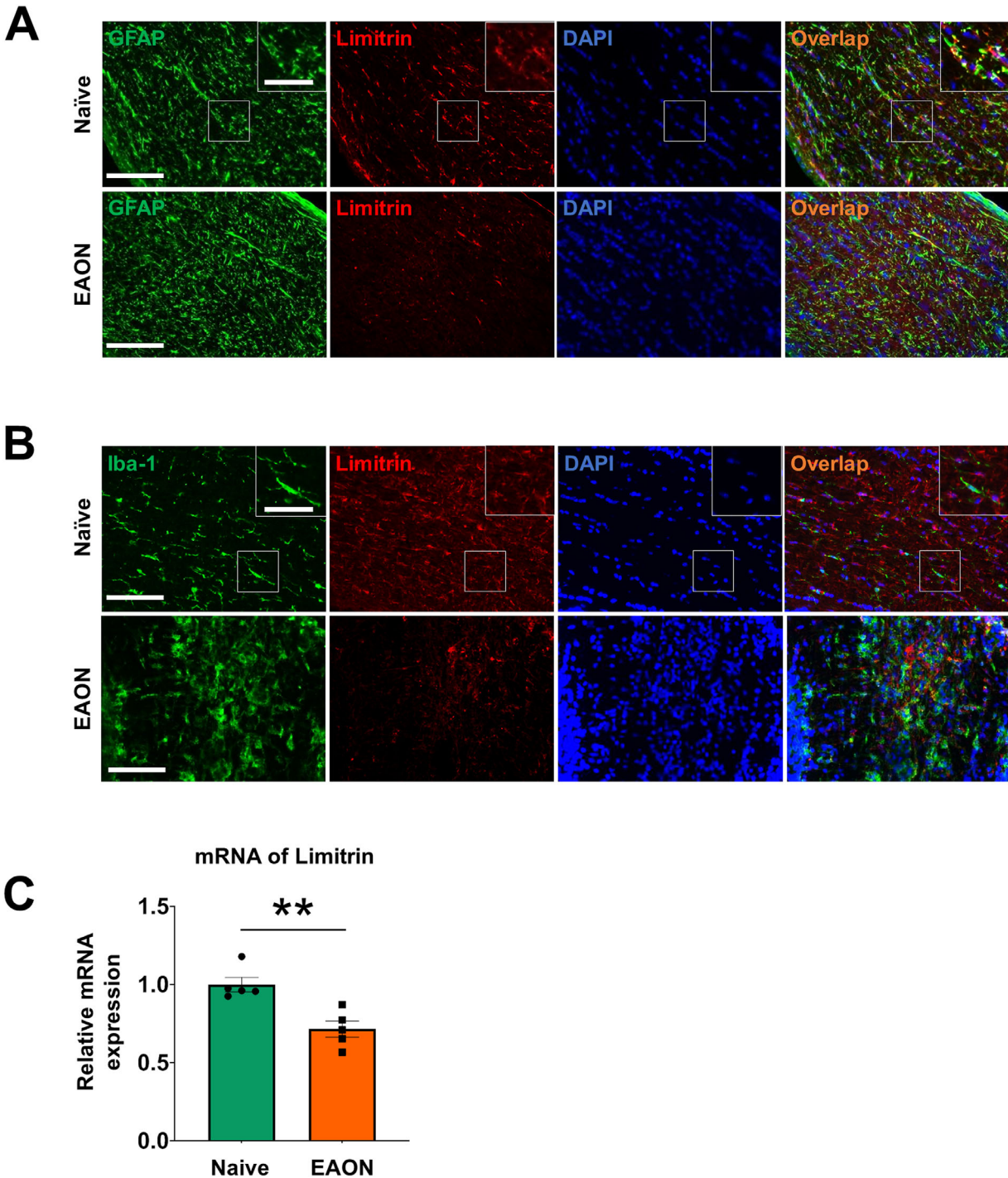


FIGURE 1. Expression and localization of limitrin in EAON-induced mice. **(A)** Immunohistochemistry of GFAP as an astrocytes-specific marker showing astrocytes (green) and limitrin (red) in the optic nerve at 17 days after immunization. **(B)** Immunohistochemical staining of Iba-1 as a microglia-specific marker showing microglia and limitrin. DAPI was used for counterstaining. Scale bar = 100 μ m (50 μ m inset). **(C)** Expression of limitrin mRNA in naïve ($n = 5$) and EAON-induced ($n = 5$) WT mice. Data are expressed as mean \pm SEM. Mann-Whitney *U* test. ** $P < 0.01$.

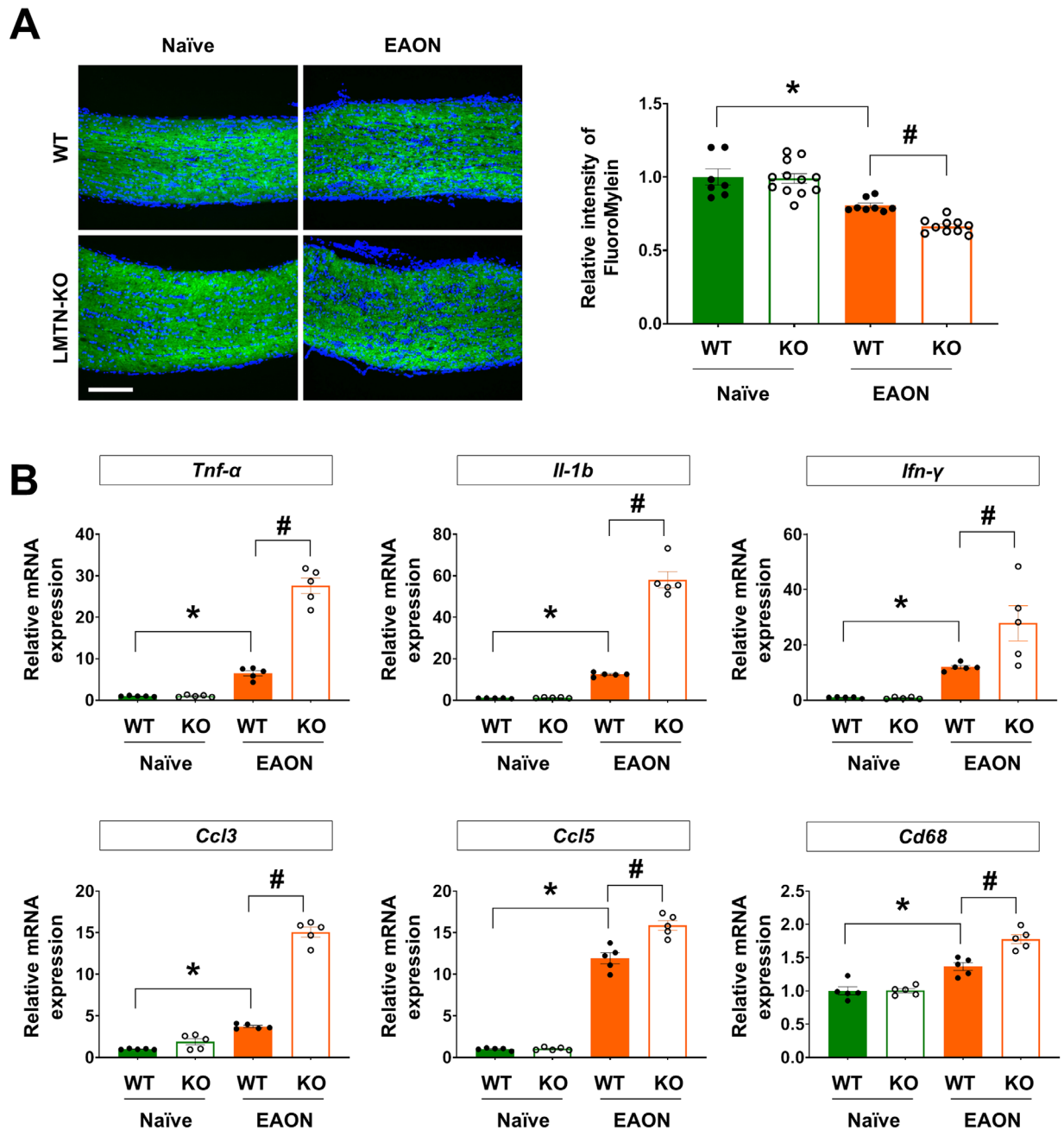


FIGURE 2. Limitrin deficiency accelerates EAON pathology. **(A)** Myelin of the optic nerve was visualized by FluoroMyelin staining in naïve (WT, $n = 7$; LMTN-KO, $n = 12$) and EAON-induced (WT, $n = 8$; LMTN-KO, $n = 10$) mice at 17 days after immunization. Scale bar = 200 μm . **(Right panel)** Quantified data of demyelination in naïve or EAON-induced WT and LMTN-KO mice. Quantification of myelin was performed by measuring the fluorescence intensity using the Fiji software. The value represents the fold-change compared with naïve WT control mice. **(B)** Expression of cytokines and chemokines in the optic nerves of naïve (WT, $n = 5$; LMTN-KO, $n = 5$) and EAON-induced (WT, $n = 5$; LMTN-KO, $n = 5$) mice at 17 days after immunization. Data are expressed as mean \pm SEM. Mann-Whitney U test. * $P < 0.05$ versus WT mice; # $P < 0.05$ versus EAON-induced mice. LMTN, limitrin.

determine the statistical significance of gene expression and fluorescence intensity. Clinical scores and categorical variables were analyzed using the Mann-Whitney nonparametric test. All other datasets were analyzed by one-way or two-way ANOVA with Bonferroni's post hoc tests. A P value of less than 0.05 was considered statistically significant.

RESULTS

Limitrin Expression Is Observed in Astrocytes in the Optic Nerve of WT Mice

To investigate a correlation between EAON and limitrin expression in the optic nerve, immunohistochemical

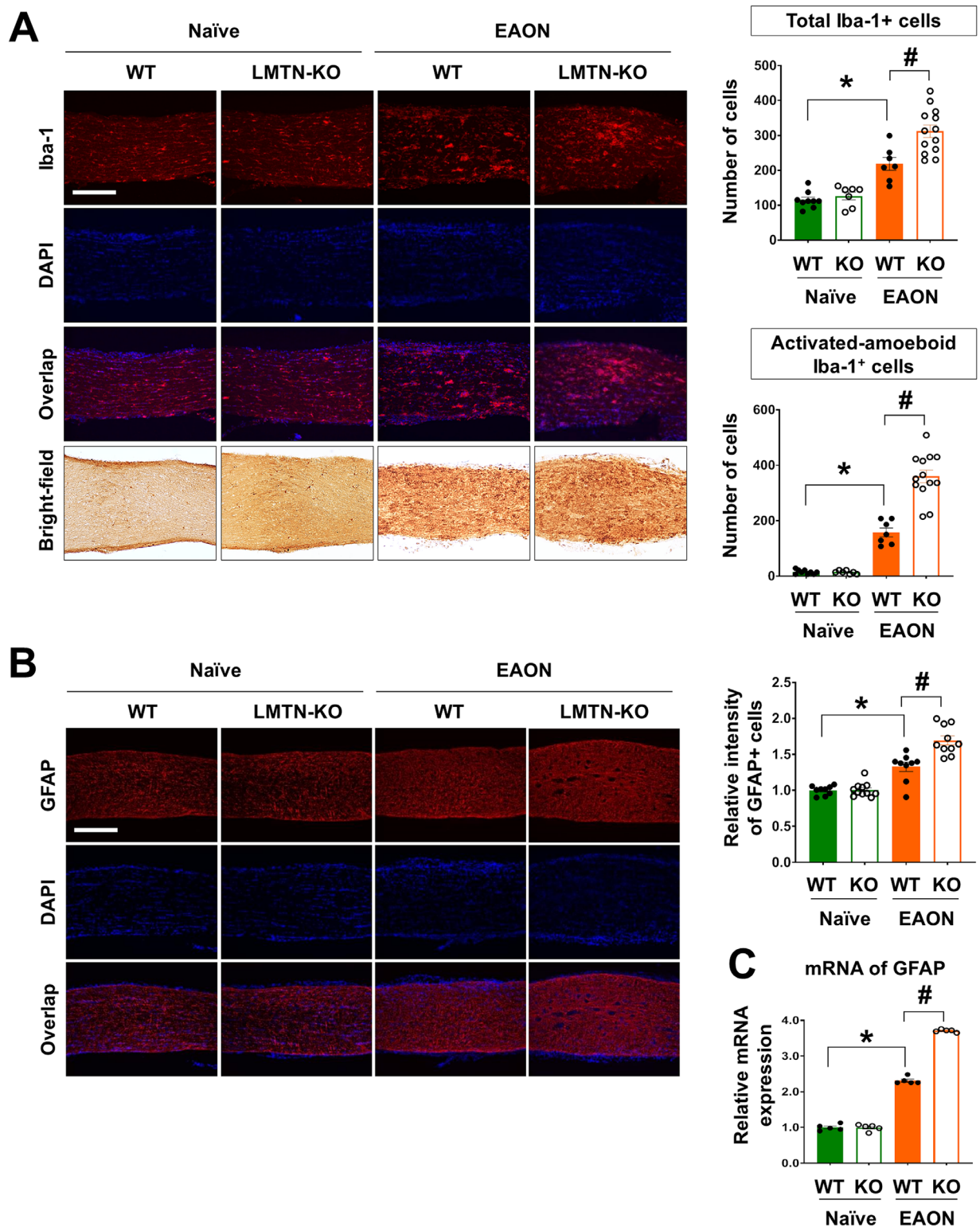


FIGURE 3. Limitrin deficiency promotes gliosis in EAON mice. **(A)** Immunofluorescence staining of Iba-1 as a microglia marker in naïve (WT, $n = 9$; LMTN-KO, $n = 7$) and EAON-induced (WT, $n = 7$; LMTN-KO, $n = 13$) mice at 17 days after immunization. (Right and upper panel) Total number of Iba-1–positive cells. (Right and lower panel) Number of amoeboid-shaped Iba-1–positive cells. **(B)** Immunofluorescence staining of GFAP as an astrocyte marker. Scale bar = 200 μ m. (Right and upper panel) Fluorescence intensity of GFAP in the optic nerve of naïve (WT, $n = 9$; LMTN-KO, $n = 7$) and EAON-induced (WT, $n = 7$; LMTN-KO, $n = 13$) mice at 17 days after immunization. Data are expressed as mean \pm SEM. **(C)** Level of GFAP mRNA expression compared between the two genotypes. Data are expressed as mean \pm SEM ($n = 5$ per each group). Mann–Whitney U test. * $P < 0.05$, naïve mice versus EAON-induced mice; # $P < 0.05$, EAON-induced WT mice versus EAON-induced LMTN-KO mice. LMTN, limitrin.

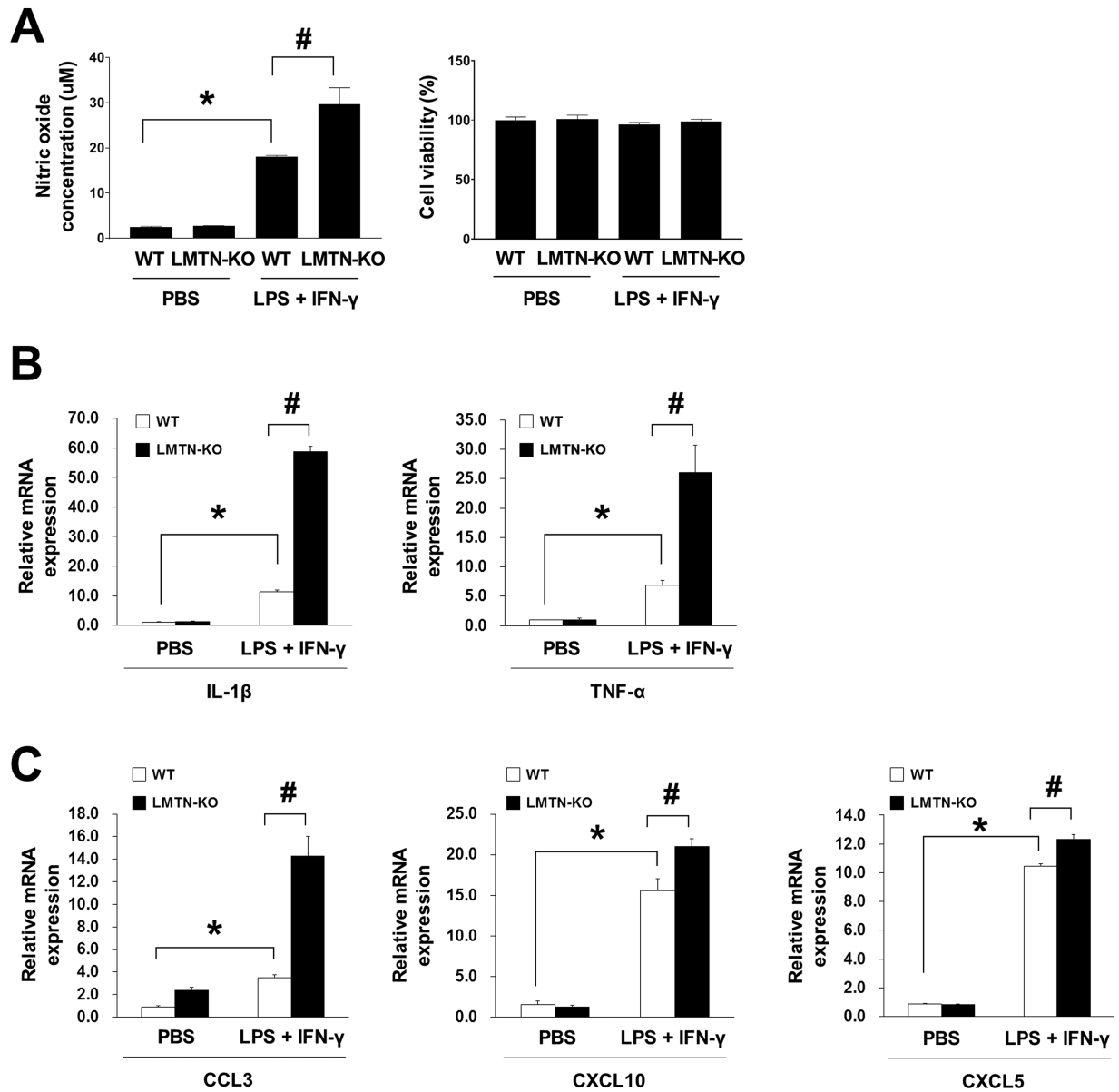


FIGURE 4. Limitrin-deficient astrocytes display greater chemotactic response to neuroinflammatory stimulation. **(A)** Results of NO assay indicating chemotactic response of astrocytes to stimulation with LPS and IFN- γ . **(B)** Expression of proinflammatory cytokines IL-1 β and TNF- α in WT or LMTN-KO astrocytes. **(C)** Expression of chemokines CCL3, CXCL10, and CXCL5, in WT or LMTN-KO astrocytes. Data are expressed as mean \pm SEM ($n = 3$ per each group). Mann-Whitney U test. * $P < 0.05$, versus control (PBS) WT astrocytes; # $P < 0.05$, versus control (PBS) LMTN-KO mice. All experiments were performed in triplicate and repeated three times. LMTN, limitrin; LPS, lipopolysaccharide.

analysis of optic nerve tissue sections was performed at day 17 after immunization with MOG, when mice showed typical grade 1 EAE symptoms. Limitrin expression was colocalized with cells stained positive for GFAP, an astrocyte-specific marker (Fig. 1A), but not with cells stained positive for Iba-1, a microglia-specific marker (Fig. 1B), indicating that limitrin was mainly expressed by astrocytes. Next, limitrin mRNA expression was compared in the optic nerves of naïve and EAON-induced WT mice (Fig. 1C), revealing that limitrin expression in EAON-induced WT mice was significantly lower than that in naïve WT mice ($P < 0.01$).

Limitrin-Deficient Mice Are More Susceptible to EAON Induction Than WT Mice

To determine the role of limitrin in EAON, optic nerve tissue sections were examined for demyelination, visualized by FluoroMyelin and hematoxylin and eosin staining. Compact myelin was observed in naïve WT and limitrin KO mice (Fig. 2A and Supplementary Fig. S2). In EAON-induced WT mice, demyelination of the optic nerve was demonstrated by partial irregularity of the linear neurofilament structure, expansion of irregularly stained axons, and

TABLE 2. Demographics and Clinical Characteristics of Patients With Optic Neuritis and Healthy Controls

	Patients With Optic Neuritis	Healthy Controls
No.	21	30
Sex (male: female)	8:13	12:18
Age (years, mean \pm SD)	38.6 \pm 15.7	36.3 \pm 12.8
Mean visual acuity at nadir (LogMAR, range)	1.1 (0.2–2.0)	NA
Mean final visual acuity (LogMAR, range)	0.1 (0–0.5)	NA
Recurrence (number, %)	9 (42.9%)	NA

NA, not applicable.

infiltrated inflammatory cells throughout the optic nerve (Fig. 2A and Supplementary Fig. S2). In the EAON-induced limitrin KO mice, demyelination of the optic nerve was significantly increased compared with that in EAON-induced WT mice ($P < 0.05$). Moreover, the expression levels of neuroinflammatory markers TNF- α , IL-1 β , IFN- γ , and CD68, and chemokines CCL3 and CCL5 were significantly increased in the optic nerves of EAON-induced limitrin KO mice compared with that in EAON-induced WT mice ($P < 0.05$) (Fig. 2B). These results indicated that limitrin KO mice experienced more severe neuroinflammation than WT mice under EAON conditions.

Limitrin Deficiency Accelerates Activation of Astrocytes and Microglia in the Optic Nerve of EAON-Induced Mice

Hyperactivation of glial cells is a hallmark of EAON.^{4,5,23,24} Immunofluorescence analysis of glia-specific markers revealed that hyperactivated astrocytes and microglia were significantly more abundant in the optic nerve after MOG immunization ($P < 0.05$) (Figs. 3A, 3B). Hyperactivation of both microglia and astrocytes was significantly greater in the optic nerves of EAON-induced limitrin KO mice than that in EAON-induced WT mice ($P < 0.05$) (Figs. 3A–C).

Limitrin-Deficient Astrocytes Display Greater Chemotactic Responsiveness Under Neuroinflammatory Stimulation

Limitrin was previously localized to astrocytic endfeet in the BBB.¹⁶ Therefore, we hypothesized that limitrin deficiency

could affect astrocytic susceptibility to neuroinflammatory stimulation, assessed by the concentration of NO released from astrocytes 48 hours after stimulation with lipopolysaccharide and IFN- γ . The NO concentration released from limitrin KO astrocytes was significantly greater than that from WT astrocytes ($P < 0.05$) (Fig. 4A). Moreover, relative mRNA expression levels of proinflammatory cytokines IL-1 β and TNF- α were significantly elevated in limitrin KO astrocytes compared with that in WT astrocytes after neuroinflammatory stimulation ($P < 0.05$) (Fig. 4B). In addition, relative mRNA expression levels of chemokines CCL3, CXCL10, and CXCL5 were significantly higher in limitrin KO astrocytes than in WT astrocytes after neuroinflammatory stimulation ($P < 0.05$) (Fig. 4C).

Increased Plasma Limitrin Levels in Patients With Optic Neuritis

Table 2 lists the demographics and clinical characteristics of patients with optic neuritis and healthy controls. Quantification of plasma limitrin levels by ELISA was performed in healthy controls ($n = 30$) and patients with optic neuritis ($n = 21$) to determine whether optic neuritis can be diagnosed by plasma limitrin levels. The mean plasma limitrin values differed significantly between the two groups (0.742 vs 2.031 ng/mL; $P = 0.0001$) and were positively correlated with LogMAR visual acuity at the nadir of the optic neuritis attack, that is, negatively correlated with visual acuity at the nadir of the optic neuritis attack ($r = 0.46$, $P = 0.036$) (Fig. 5).

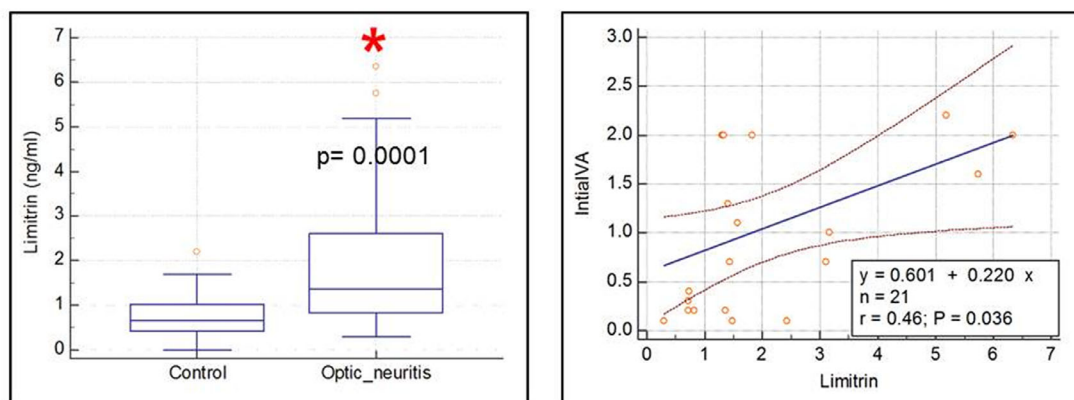


FIGURE 5. Increased plasma limitrin levels in patients with optic neuritis. Left panel, quantification of plasma limitrin levels by ELISA in healthy controls ($n = 30$) and patients with optic neuritis ($n = 21$). Mann–Whitney U test. $P = 0.0001$. Right panel, correlation between mean plasma limitrin level and LogMAR visual acuity at the nadir of the optic neuritis attack. ($r = 0.46$, $P = 0.036$).

DISCUSSION

The current study localized limitrin expression in astrocytes in the optic nerve of WT mice and revealed that limitrin expression was downregulated in EAON-induced WT mice. Further, limitrin KO mice were more susceptible to EAON induction than WT mice, as indicated by significantly increased demyelination, enhanced expression of proinflammatory cytokines TNF- α , IL-1 β , IFN- γ , and CD68, and chemokines CCL3 and CCL5, and greater reactive gliosis in the optic nerves after EAON induction. All of these factors have the capacity to contribute to BBB disruption and immune cell infiltration, suggesting that limitrin may play a protective role against neuroinflammation and reactive gliosis by decreasing immune cell infiltration into the CNS. These results are consistent with those of Yonezawa et al.,¹⁶ who reported that limitrin expression was downregulated when the BBB was destroyed owing to cold injury correlating with BBB disruption, and restored to control levels after injury repair. These results strongly suggest that limitrin is a component of the BBB that may be required for its maturation and maintenance. Therefore, decreased limitrin expression in the optic nerve owing to EAON induction may reflect BBB disruption by neuroinflammation.

Limitrin-deficient astrocytes displayed significantly increased expression levels of proinflammatory cytokines TNF- α , and IL-1 β , and chemokines CCL3, CXCL10, and CXCL5 after neuroinflammatory stimulation than WT astrocytes. These results concur with those of previous studies in which IL-1 β modulated BBB permeability in mice/rats and activated human endothelial cells.^{28,29} IL-1 β is a cytokine produced by T helper 17 cells that can enhance BBB disruption and recruit neutrophils into the CNS.^{30,31} Studies reported that IL-1 β activates microglia and astrocytes, further stimulating demyelination.^{32,33} CXCL10 is a chemokine that attracts activated T cells and is present at higher concentration in the cerebrospinal fluid of patients with active MS.^{14,34} Cramer et al.¹⁴ reported that BBB permeability was correlated with CXCL10 concentrations in the cerebrospinal fluid of patients with optic neuritis. Therefore, the loss of BBB integrity induced by limitrin deficiency may accelerate the influx of peripheral immune cells into the optic nerve, resulting in proinflammatory conditions.

One of the notable findings of this study is that patients with optic neuritis demonstrated higher plasma limitrin levels than healthy controls, which was correlated with worse visual loss at the nadir of the optic neuritis attack. These results suggest that the secretion of limitrin into the plasma from its origin may reflect a loss of its normal physical and functional barrier function to the BBB, induced by optic neuritis. Moreover, limitrin may be cleaved by proteases during BBB disruption, such as matrix metalloprotease 9. Recent studies demonstrated that the extent of BBB disruption was correlated with the severity of CNS neuroinflammatory diseases such as MS and neuromyelitis optica.^{14,20} The onset of optic neuritis results from the entry of T cells into the optic nerve through the disrupted BBB, allowing proinflammatory factors and leukocytes to invade the retina or optic nerve, which results in neuroinflammation that leads to decreased vision.^{14,18,20} Therefore, we suggest that plasma limitrin levels in patients with optic neuritis may reflect the extent of BBB disruption owing to optic neuritis.

Our future work will focus on the correlation between the extent of BBB disruption observed via MRI and plasma limitrin levels. In addition, we will investigate the molecular

mechanism of limitrin proteolysis and possible correlations between plasma limitrin levels and the final visual outcomes or recurrence rates in patients with optic neuritis.

In conclusion, the results of the current study demonstrate that limitrin deficiency induces severe neuroinflammation and reactive gliosis in the optic nerve after EAON induction. Our results imply that astrocyte-derived limitrin may play a protective role against neuroinflammation by reducing infiltration of peripheral immune cells into the CNS. Considering that patients with higher plasma limitrin levels demonstrated worse visual loss at the nadir of the optic neuritis attack, plasma limitrin level may provide a potentially valuable biomarker of disease severity in patients with optic neuritis.

Acknowledgments

Supported by the National Research Foundation of Korea Grant funded by the Korean Government (2018R1A2B6008685 and 2020R111A1A01070926).

Disclosure: **B.Y. Chun**, None; **J.-H. Kim**, None; **Y.-K. Jung**, None; **Y.S. Choi**, None; **G. Kim**, None; **T. Yonezawa**, None; **K. Suk**, None

References

1. Arnold AC. Evolving management of optic neuritis and multiple sclerosis. *Am J Ophthalmol.* 2005;139(6):1101–1108.
2. Beck RW, Trobe JD, Moke PS, et al. High- and low-risk profiles for the development of multiple sclerosis within 10 years after optic neuritis: experience of the optic neuritis treatment trial. *Arch Ophthalmol.* 2003;121(7):944–949.
3. Beck RW, Gal RL, Bhatti MT, et al. Visual function more than 10 years after optic neuritis: experience of the optic neuritis treatment trial. *Am J Ophthalmol.* 2004;137(1):77–83.
4. Shindler KS, Ventura E, Dutt M, Rostami A. Inflammatory demyelination induces axonal injury and retinal ganglion cell apoptosis in experimental optic neuritis. *Exp Eye Res.* 2008;87(3):208–213.
5. Matsunaga Y, Kezuka T, An X, et al. Visual functional and histopathological correlation in experimental autoimmune optic neuritis. *Invest Ophthalmol Vis Sci.* 2012;53(11):6964–6971.
6. Kornnek B, Storch MK, Weissert R, et al. Multiple sclerosis and chronic autoimmune encephalomyelitis: a comparative quantitative study of axonal injury in active, inactive, and remyelinated lesions. *Am J Pathol.* 2000;157(1):267–276.
7. Frohman EM, Racke MK, Raine CS. Multiple sclerosis—the plaque and its pathogenesis. *N Engl J Med.* 2006;354(9):942–955.
8. Remington LT, Babcock AA, Zehntner SP, Owens T. Microglial recruitment, activation, and proliferation in response to primary demyelination. *Am J Pathol.* 2007;170(5):1713–1724.
9. Ponomarev ED, Shriver LP, Maarek K, Dittel BN. Microglial cell activation and proliferation precedes the onset of CNS autoimmunity. *J Neurosci Res.* 2005;81(3):374–389.
10. Zlokovic BV. The blood-brain barrier in health and chronic neurodegenerative disorders. *Neuron.* 2008;57(2):178–201.
11. Bennett JJ, Basivireddy A, Kollar KE, et al. Blood-brain barrier disruption and enhanced vascular permeability in the multiple sclerosis model EAE. *J Neuroimmunol.* 2010;229(1-2):180–191.
12. Popescu BF, Lucchinetti CF. Pathology of demyelinating diseases. *Annu Rev Pathol.* 2012;7:185–217.

13. Aube B, Levesque SA, Pare A, et al. Neurophils mediate blood-spinal cord barrier disruption in demyelinating neuroinflammatory diseases. *J Immunol*. 2014;193(5):2438–2454.
14. Cramer SP, Modvig S, Simonsen HJ, Frederiksen JL, Larsson HBW. Permeability of the blood-brain barrier predicts conversion from optic neuritis to multiple sclerosis. *Brain*. 2015;138(Pt 9):2571–2583.
15. Guy J, McGorray S, Fitzsimmons J, et al. Reversals of blood-brain barrier disruption by catalase: a serial magnetic resonance imaging study of experimental optic neuritis. *Invest Ophthalmol Vis Sci*. 1994;35(9):3456–3465.
16. Yonezawa T, Ohtsuka A, Yoshitaka T, et al. Limitrin, a novel immunoglobulin superfamily protein localized to glia limitans formed by astrocyte endfeet. *Glia*. 2003;44(3):190–204.
17. Peters A, Palay SL, Webster HDF. *The Fine Structure of the Nervous System, Neurons and Their Supporting Cells*. New York: Oxford University Press. 1991:344–355, 395–406.
18. Broux B, Gowing E, Prat A. Glial regulation of the blood-brain barrier in health and disease. *Semin Immunopathol*. 2015;37(6):577–590.
19. Prat A, Biernacki K, Wosik K, et al. Glial cell influence on the human blood-brain barrier. *Glia*. 2001;36(2):145–155.
20. Liang S, Qin Q, Tang Y, Liao W, Yang Y, He J, Li L. Impact of blood-brain barrier disruption on newly diagnosed neuromyelitis optica spectrum disorder symptoms and prognosis. *Ann Palliat Med*. 2020;9(2):324–330.
21. Jung YK, Jin JS, Jeong JH, et al. DICAM, a novel dual immunoglobulin domain containing cell adhesion molecule interacts with $\alpha\beta 3$ integrin. *J Cell Physiol*. 2008;216(3):603–614.
22. Han SW, Kim JM, Lho Y, et al. DICAM attenuates experimental colitis via stabilizing junctional complex in mucosal barrier. *Inflamm Bowel Dis*. 2019;25(5):853–861.
23. Kesuka T, Usui Y, Goto H. Analysis of the pathogenesis of experimental autoimmune optic neuritis. *J Biomed Biotechnol*. 2011;2011:294046, <https://doi.org/10.1155/2011/294046>.
24. Chun BY, Kim JH, Nam Y, Huh MI, Han S, Suk K. Pathological involvement of astrocyte-derived lipocalin-2 in the demyelinating optic neuritis. *Invest Ophthalmol Vis Sci*. 2015;56:3691–3698.
25. Larabee CM, Hu Y, Desai S, et al. Myelin-specific Th17 cells induce severe relapsing optic neuritis with irreversible loss of retinal ganglion cells in C57BL/6 mice. *Mol Vis*. 2016;22:332–341.
26. Wada M, Yoshimi K, Higo N, Ren YR, Mochizuki H, et al. Statistical parametric mapping of immunopositive cell density. *Neurosci Res*. 2006;56(1):96–102.
27. Kerstetter AE, Miller RH. Isolation and culture of spinal cord astrocytes. *Methods Mol Biol*. 2012;814:93–104.
28. Zhu W, London NR, Gibson CC, Davis CT, Tong Z, et al. Interleukin receptor activates a MYD88-ARNO-ARF6 cascade to disrupt vascular stability. *Nature*. 2012;492(7428):252–255.
29. Argaw AT, Zhang Y, Snyder BJ, Zhao ML, Kopp N, et al. IL-1 β regulates blood-brain barrier permeability via reactivation of the hypoxia-angiogenesis program. *J Immunol*. 2006;177(8):5574–5584.
30. Sutton C, Brereton C, Keogh B, Mills KH, Lavelle EC. A crucial role for interleukin-1 in the induction of IL-17 producing T cells that mediate autoimmune encephalomyelitis. *J Exp Med*. 2006;203(7):1685–1691.
31. Stockinger B, Veldheon M. Differentiation and function of Th17 T cells. *Curr Opin Immunol*. 2007;19(3):281–286.
32. Balasa R, Barcutean L, Balasa A, Motatianu A, Roman-Filip C, Manu D. The action of Th17 cells on blood brain barrier in multiple sclerosis and experimental autoimmune encephalomyelitis. *Hum Immunol*. 2020;81(5):237–243.
33. Ferrati CC, Depino AM, Prada F, et al. Reversible demyelination, blood-brain barrier breakdown, and pronounced neutrophil recruitment induced by chronic IL-1 expression in the brain. *Am J Pathol*. 2004;165(5):1827–1837.
34. Sorensen TL, Sellebjerg F, Jensen CV, Strieter RM, Ransohoff RM. Chemokines CXCL10 and CCL2: differential involvement in intrathecal inflammation in multiple sclerosis. *Eur J Neurol*. 2001;8(6):665–672.